SYNTHESIS OF PRECURSOR-DERIVED TiC-Ni BASED NANOCOMPOSITES BY DIRECT REDUCTION & CARBURIZATION PROCESSING

Ji-ren Xie[1], Xing-long Duan[1], Gang-qin Shao[1,2], Zhong-lai Yi[1], Jia Li[1], Run-zhang Yuan[1] and Jing-kun Guo[1,2]

[1]State Key Laboratory of Advanced Technology for Materials Synthesis & Processing, Wuhan University of Technology, 122 Luoshi Road, Wuhan 430070, P. R. China
[2]Shanghai Institute of Ceramics, Chinese Academy of Science, 1295 Dingxi Road, Shanghai 200050, P. R. China

Abstract. Precursor-derived TiC-Ni and TiC-Cr_3C_2-Ni nanocomposites were synthesized by direct reduction and carburization processing. This improved carbothermal synthesis technology has proven very versatile as a wider range of compositions can be produced. Their phase structure, morphological feature and particle size were characterized by XRD and SEM. Results show that the interfacial bonding between TiC and Ni was found to be of a good quality. The TiC reinforcement was in situ formed instead of being added to the matrix. The formation mechanism of the TiC-Ni and TiC-Cr_3C_2-Ni nanocomposites was discussed.

1. INTRODUCTION

Cemented carbides or hardmetals (cermets) based on tungsten carbide (WC) and titanium carbide (TiC) have reached a considerable degree of property refinement. TiC is a very attractive ceramic material because of its high melting point (3260 °C), low density (4.93 g·cm^{-3}), extreme hardness (Knoop's = 32.4 GPa; H_v = 3200) and strength, excellent wear resistance, low friction coefficient, high thermal conductivity (16.7 W·m^{-1}·K^{-1}), high thermal shock resistance, high electrical conductivity (30·10^{-6} Ω·cm), high chemical stability, capacity to deform plastically at high temperatures in a manner similar to fcc metals and high solvency for other carbides [1]. TiC based cermets (TiC-Ni is the commonest) have drawn much attention as a promising candidate for the high performance WC-Co cutting tools [2-4]. They have a large number of applications such as cutting tools, drill bits, wire drawing dies, punch and die sets, spray and blast nozzles, aluminum and plastic extrusion dies, etc. [5,6].

For all these applications and to achieve a fine microstructure, the synthesis of TiC powders with a homogeneous chemical composition, fine particle, a narrow particle size distribution, and a loose agglomeration is of great importance. Methods that have been developed to synthesize TiC and TiC-Ni powders include the direct carbonization of titanium metal (combustion synthesis, reaction synthesis) [7,8] or titanium hydride [9], mechanical alloying [10], self-propagating high-temperature synthesis [11], gaseous pyrolysis of titanium halide [12], gas-phase laser-induced reaction [13], spark crosion [14], spark discharge [15], melt-infiltration process [16], insolvent metals process [17,18] and carbothermal synthesis [19-22].

In the carbothermal synthesis of TiC from a mixture of TiO_2 and C powder, the overall reaction governing the formation of TiC is

$$TiO_2 + 3C = TiC + 2CO \text{ (g)}. \qquad (1)$$
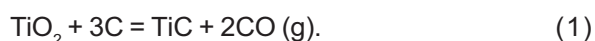
The reaction is highly endothermic and proceeds above 1289 °C for a partial pressure of CO below
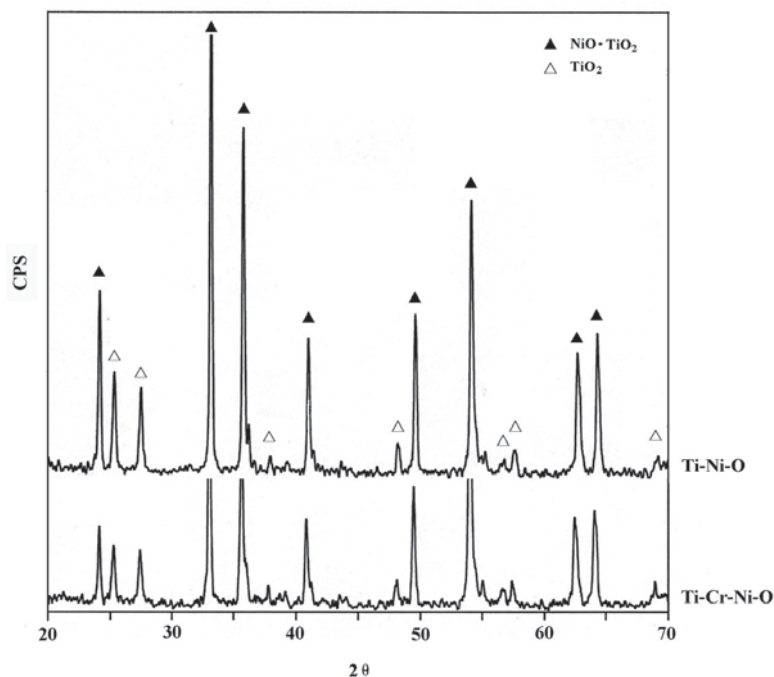

Fig. 1. XRD patterns of Ti-Ni-O and Ti-Cr-Ni-O composite oxide powders (▲ NiO·TiO$_2$; △ TiO$_2$).

1.013·10^5 Pa [19]. However, the actual TiC production is achieved at much higher temperatures than the thermodynamic onset temperature because of kinetic barriers such as limited contact area between reactants and uneven distribution of carbon in the reactants. For example, in the commercial production, reactants are fired at 1900 °C to 2300 °C in an inert atmosphere while sintered lumps of TiC are produced.

In this study, the precursor-derived/direct reduction-carburization process is used as an improved carbothermal synthesis technology to produce TiC-Ni and TiC-Cr$_3$C$_2$-Ni nanocomposite powder. Such a method would possess advantages that the separate production of Ni powder and the subsequent mixing with TiC powder (or other carbides) could be obviated. The objective of this study is to investigate the synthesizing behavior of the powders, and evaluate their microstructure and grain morphology.

2. EXPERIMENTAL PROCEDURES

For TiC-30Ni vol.% synthesis, the liquid titanium tetrachloride and aqueous nickel nitrate reacted to form a transparent sol, while the pH value (was adjusted by adding ammonia), the concentration of the solution, the reactive temperature and time were controlled. The clear sol was dehydrated at 110 °C to yield a gel powder (precursor). Then the precursor was heat-treated to become nanocomposite oxide powder at 800 °C for 0.5 h in air. After that, the as-fabricated nanocomposite oxide powder was ball-milled with fine carbon powder in aceton, then fired to form TiC-Ni powder at 1550 °C for 2 h under flowing nitrogen gas.

For TiC-0.5Cr$_3$C$_2$-30Ni vol.% synthesis, the liquid titanium tetrachloride, aqueous nickel nitrate and aqueous (NH$_4$)$_2$Cr$_2$O$_7$ reacted to form a transparent sol. Other reactive conditions were the same as above, not including the fire temperature was 1580 °C and fire time was 2 h or 3 h.

The specific surface area of nanocomposite oxide powders were determined by a BET analyzer. The phase structure of nanocomposite oxide powders and carbide powders were studied by XRD. The grain morphology of the samples were analyzed by SEM.

3. RESULTS AND DISCUSSION

XRD patterns of Ti-Ni-O and Ti-Cr-Ni-O composite oxide powders are shown in Fig. 1. The diffraction peaks of NiO·TiO$_2$ and TiO$_2$ were detected from both samples. No diffraction peaks is observed that can be attributed to chromium oxide because chromium element has a low content. It could be concluded that the NiO decomposed from nickel nitrate reacts with TiO$_2$ (produced by the hydrolyzing of TiCl$_4$) to

**Table 1.** Specific surface area and equivalent particle size of the composite oxide powders.

No.	Sample	BET multipoint specific surface area (m²/g)	d_{BET} (nm)	ρ_{th} (g/cm³)
1	Ti-Ni-O	69.5457	15	5.618
2	Ti-Cr-Ni-O	12.2336	87	5.627

form $NiO \cdot TiO_2$. The $NiO \cdot TiO_2 / TiO_2$ powders synthesized therefrom have a homogeneous nanocrystalline structure.

The specific surface area and equivalent particle size of the as-fabricated composite oxide powders are summarized in Table 1. The specific surface area of Ti-Ni-O composite oxide powder is 69.5457 m²/g and the corresponding mean particle size is about 15 nm. And the specific surface area of Ti-Cr-Ni-O composite oxide powder is 12.2336 m²/g while the corresponding mean particle size is about 87 nm.

Fig. 2 shows the phases analysis result of (Ti-C)-Ni and (Ti-Cr-C)-Ni composite powders. After the mixture of Ti-Ni-O composite oxide powder and fine carbon powder fired at 1550 °C for 2 h under flowing nitrogen gas, all of the phases detected in the sample are TiC and Ni phases (unreacted carbon was detected in all of the fired samples, not discussed in
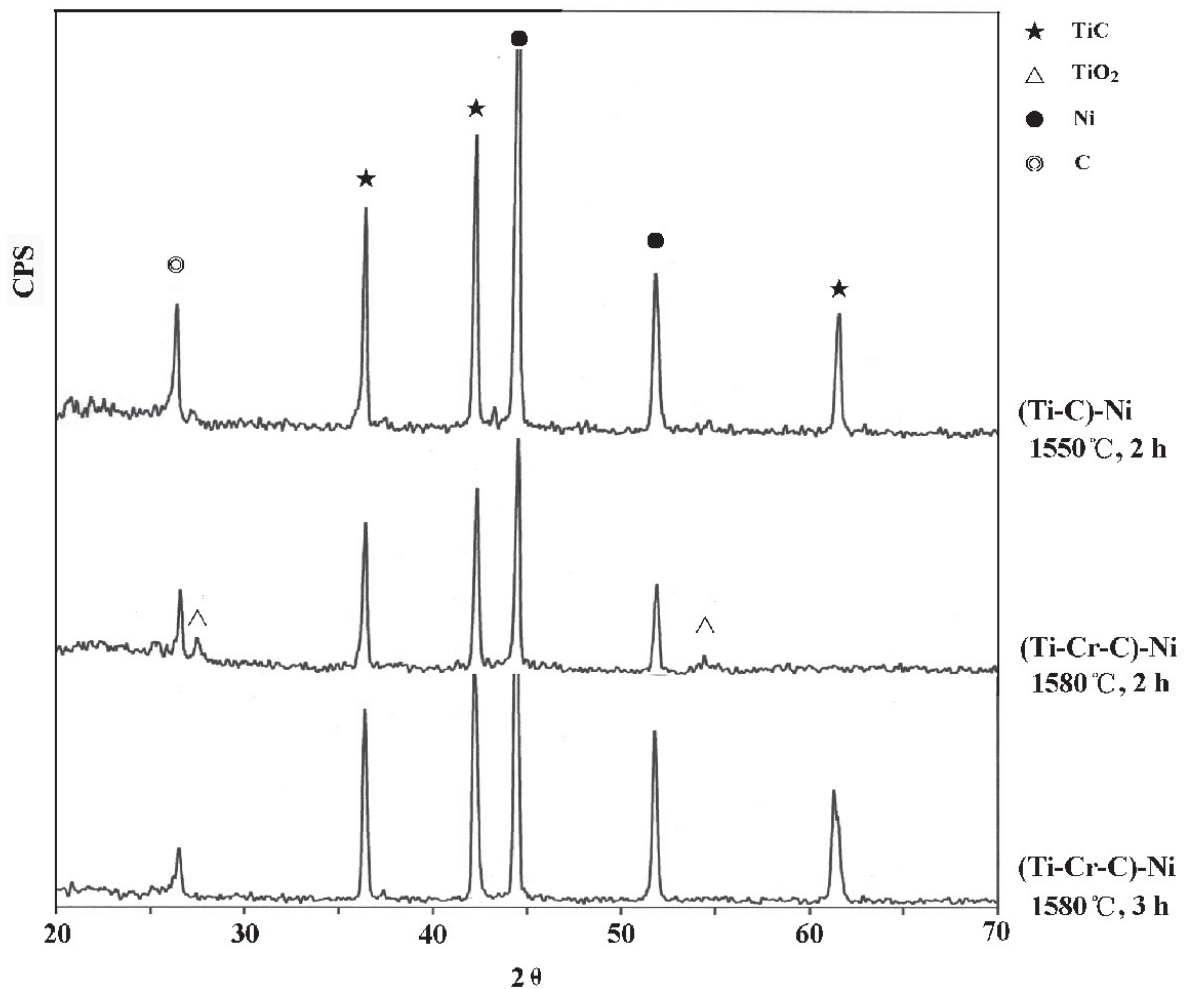
Fig. 2. XRD pattern of (Ti-C)-Ni and (Ti-Cr-C)-Ni composite powders (★ TiC; △ TiO_2; ● Ni; ◎ free C). (a) – (Ti-C)-Ni composite powder (1550 °C, 2h); (b) – (Ti-Cr-C)-Ni composite powder (1580 °C, 2h); (c) – (Ti-Cr-C)-Ni composite powder (1580 °C, 3h).
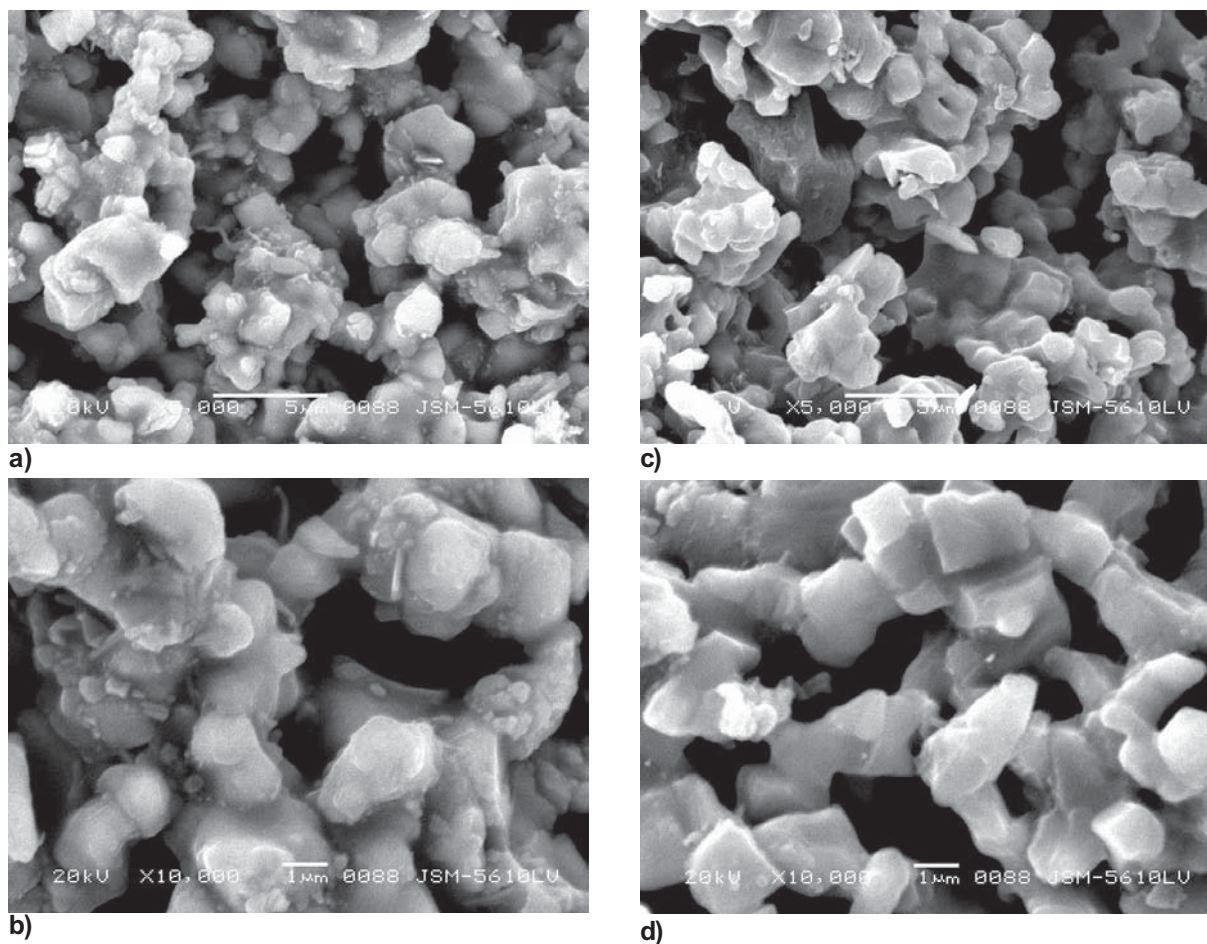
Fig. 3. SEM micrographs of TiC-Ni and TiC-Cr$_3$C$_2$-Ni composite powders. (a), (b) – TiC-Ni composite powder (1550 °C, 2h); (c), (d) – TiC-Cr$_3$C$_2$-Ni composite powder (1580 °C, 3h).

this paper in detail). For the sample of mixture of Ti-Cr-Ni-O powder and C powder, the TiO$_2$ peaks still exist after it was fired at 1580 °C for 2 h. But when it was fired at 1580 °C for 3 h, TiO$_2$ peaks disappear and all of the detected peaks are of the synthesized TiC and Ni. No chromium oxide or chromium carbide diffraction peaks are observed in the fired sample of mixture of Ti-Cr-Ni-O powder and C powder. This is still due to that the chromium element has a low content. Considering that Cr$_3$C$_2$ can be formed more easily than TiC when they are in the same thermodynamic condition, chromium carbide but not chromium oxide phase should be in the fired sample (1580 °C, 3 h) of mixture of Ti-Cr-Ni-O powder and C powder. All of the above results meant that formation temperature of the TiC fabricated by using precursor-derived/direct reduction-carburization process is about 100 °C lower than that by using classical process (over 1700 °C).

The phase diagram of the ternary Ni–Ti–C system has been studied by other authors [23,24]. An analysis of the literature shows that above 1295 °C it is possible to create a liquid solution of Ni–Ti–C and close to the Ni corner in Ni–Ti–C system there are two ternary eutectics. Moreover, a pseudo-binary TiC–Ni system is a typical eutectic system [25].

Upon above consideration, that the carbothermal synthesis of (Ti-C)-Ni and (Ti-Cr-C)-Ni composite powders follows the scheme can be concluded as Eq. (1) and the following:

$$TiO_2 \cdot NiO + 4C = TiC + Ni + 3CO(g), \qquad (2)$$

$$3Cr_2O_3 + 13C = 2Cr_3C_2 + 9CO(g). \qquad (3)$$
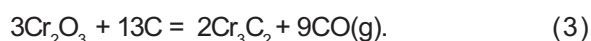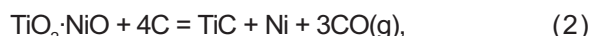
The morphology of TiC-Ni composite powder synthesized at 1550 °C for 2 h under flowing nitrogen gas is shown in Figs. 3a and 3b. The TiC-Ni composite powder has a fine particle size (0.5-1

μm) and is agglomerated. The morphology of TiC-Cr_3C_2-Ni composite powder synthesized at 1580 °C for 3 h under flowing nitrogen gas is shown in Figs. 3c and 3d. The TiC-Cr_3C_2-Ni composite powder has a fine particle size (0.5-1 μm) and is moderately agglomerated. It is obvious that the addition of Cr_3C_2 is propitious to the refinement of TiC grain.

4. CONCLUSIONS

In the Ti-Ni-O and Ti-Cr-Ni-O nanocomposite oxide powders, nickel element exists in the form of $NiO \cdot TiO_2$.

The formation temperature of TiC fabricated using precursor-derived/direct reduction-carburization process is about 100 °C lower than that typical for conventional process.

ACKNOWLEDGEMENTS

REFERENCES

[1] R. Kamo, *Engineered Materials Handbook, vol.4* (ASM International, Materials Park, PA, 1994).

[2] G. Q. Shao, B. L. Wu, X. L. Duan, J. R. Xie, M. K. Wei and R. Z. Yuan, In: *Innovative Processing / Synthesis: Ceramics, Glasses, Composites IV*, ed. by N. P. Bansal and J. P. Singh (The American Ceramic Society: Ohio, USA, 2000) p.375.

[3] H.S. Kalish // *Met. Prog.* **124** (1983) 21.

[4] D. Moskowitz // *US Patent 4,108,694, August 22, 1978*.

[5] Kenneth J. A. Brookes, *World Directory and Handbook of Hardmetals and Hard Materials, 5th Edition* (MPR Publishing Services Ltd, Old Bank Buildings, Shrewsbury SY1 1HU, England, 1991).

[6] P. F. Becher and K. P. Plucknett // *J. Euro. Ceram. Soc.* **18** (1997) 395.

[7] D. C. Halverson, K. H. Ewald and Z. A. Munir // *J. Mater. Sci.* **28** (1993) 4583.

[8] B. L. Jong // *Scripta Materialia* **37** (1997) 1979.

[9] I. N. Mihailescu, M. L. De Giorge, C. H. Boulmer-Leborgne and S. Urdea // *J. Appl. Phys.* **75** (1994) 5286.

[10] C.-J. Choi // *J. Mater. Proc. Technol.* **104** (2000) 127.

[11] J. C. Lasalvia and M. A. Meyers // *Int. J. Self-Propagating High-Temper. Syn.* **4** (1995) 43.

[12] D. D. Harbuck, C. F. Davidson and B. Monte // *J. Metals* **38** (1986) 47.

[13] R. Alexandrescu // *J. Mater. Sci.* **32** (1997) 5629.

[14] M. S. Husu // *Script Metall. Mater.* **32** (1995) 805.

[15] S. Tsuglo // *British Ceram. Trans.* **94** (1995) 250.

[16] K. P. Plucknett, P. F. Becher and R. Subramanian // *J. Mater. Res.* **12** (1997) 2515.

[17] G. Cliché // *Mater. Sci. & Eng. A* **32** (1991) 5629.

[18] S. Y. Ahn and S. Kang // *J. Am. Ceram. Soc.* **83** (2000) 6.

[19] R. Koc // *J. Mater. Sci.* **33** (1998) 1049.

[20] R. Koc and J. S. Folmer // *J. Mater. Sci.* **32** (1997) 3101.

[21] R. Koc, C. Meng and G.A. Swift // *J. Mater.* **35** (2000) 3131.

[22] G. A. Swift and R. Koc // *Ceram. Trans.* **108** (1999) 43.

[23] W. C. Ballamy and E. E. Hucke // *J. Metals* **22** (1970) 43.

[24] E. R. Stover and J. Wulff // *Trans. AIME* **215** (1959) 127.

[25] H. Frey and H. Holleck, In: *Handbook of Ternary Alloy Phase Diagrams, vol. 6*, ed. by P. Villars, A. Prince and H. Okamoto (ASM International: Materials Park, OH, 1995) p. 7246.